PHYSICAL REVIEW B **96**, 041407(R) (2017)

Solvent fluctuations and nuclear quantum effects modulate the molecular hyperpolarizability of water

Chungwen Liang,[1,2,*] Gabriele Tocci,[1,2] David M. Wilkins,[1,2] Andrea Grisafi,[1] Sylvie Roke,[2] and Michele Ceriotti[1]

[1]*Laboratory of Computational Science and Modeling, Institute of Materials, École Polytechnique Fédérale de Lausanne, CH-1015 Lausanne, Switzerland*

[2]*Laboratory for Fundamental BioPhotonics (LBP), Institute of Bioengineering (IBI), Institute of Materials Science (IMX), School of Engineering (STI), and Lausanne Centre for Ultrafast Science (LACUS), École Polytechnique Fédérale de Lausanne, CH-1015 Lausanne, Switzerland*

(Received 9 February 2017; revised manuscript received 3 July 2017; published 20 July 2017)

Second-harmonic scattering (SHS) experiments provide a unique approach to probe noncentrosymmetric environments in aqueous media, from bulk solutions to interfaces, living cells, and tissue. A central assumption made in analyzing SHS experiments is that each molecule scatters light according to a constant molecular hyperpolarizability tensor $\boldsymbol{\beta}^{(2)}$. Here, we investigate the dependence of the molecular hyperpolarizability of water on its environment and internal geometric distortions, in order to test the hypothesis of constant $\boldsymbol{\beta}^{(2)}$. We use quantum chemistry calculations of the hyperpolarizability of a molecule embedded in point-charge environments obtained from simulations of bulk water. We demonstrate that both the heterogeneity of the solvent configurations and the quantum mechanical fluctuations of the molecular geometry introduce large variations in the nonlinear optical response of water. This finding has the potential to change the way SHS experiments are interpreted: In particular, isotopic differences between H_2O and D_2O could explain recent SHS observations. Finally, we show that a machine-learning framework can predict accurately the fluctuations of the molecular hyperpolarizability. This model accounts for the microscopic inhomogeneity of the solvent and represents a step towards quantitative modeling of SHS experiments.

DOI: 10.1103/PhysRevB.96.041407

Nonlinear optical (NLO) processes are of great interest in physics, chemistry, biology, and materials science, as they provide a means of probing the structure and behavior of liquids, nanostructures, and interfaces [1,2]. Second-harmonic generation (SHG) is a NLO process in which two photons with frequency ω are instantaneously combined to generate a new photon with frequency 2ω after interacting with a material. As a second-order NLO process, SHG is only allowed in noncentrosymmetric environments. SHG spectroscopy experiments in molecular systems can be carried out in three different geometries: reflection, transmission, and scattering (SHS) [3–5]. The properties of planar interfaces are often probed by SHG spectroscopy in the reflection mode, while the properties of spherical interfaces and bulk materials are often probed by SHG spectroscopy in the scattering mode [6,7]. The structural information of molecular systems, such as molecular adsorption and orientation on metal surfaces [3,8], polarity of liquid interfaces [9], nanoparticles in solutions [10,11] and bulk molecular liquids [12], has been intensively studied by SHG spectroscopy.

Theoretical frameworks for the estimation of the SHG response in the reflection and scattering modes have long been known [5,13,14], and are necessary to interpret experimental results. The SHG response of a molecular system simultaneously carries information on the structural correlations and the nonlinear optical response of each molecule, and modeling is required to disentangle these contributions to the experimental measurements [15]. However, it is challenging to do so without introducing limiting approximations. For instance, to extract information on orientational correlations at interfaces or in the bulk phase, it is common to assume that scattering from molecules in solution is incoherent [6,9,16]. However, recent experiments and simulations have found evidence of a significant coherent contribution to the scattering, particularly in the case of hydrogen-bonded solvents. [17–20] Another critical assumption that is often made is that the hyperpolarizability tensor $\boldsymbol{\beta}^{(2)}$ of the molecules is constant, independent of the environment and the molecular geometries. Most experimental analyses rely on electronic structure calculations to obtain an estimate of $\boldsymbol{\beta}^{(2)}$. Early computational studies focused on calculating this microscopic quantity for gas-phase molecules [21–23], while more recently the role of solvation has also been considered [24–26].

Due to its ubiquitous presence in chemical and biological systems, water has been given special attention in experimental and theoretical SHS studies. As a consequence of the strong electrostatic interactions in the liquid, the electronic structure of water and therefore its molecular hyperpolarizability change significantly on going from the gas phase to the liquid phase [27,28]. To determine these changes quantitatively, several quantum chemistry calculations have been performed based on simple point-charge environments [26], dielectric continuum theories [29], solvation models [30], and mixed quantum/classical (QM/MM) approaches [29,31] to incorporate the environmental effect. Even though the value of the hyperpolarizability is very sensitive to the level of theory, functional, and basis set, all of these studies report a sign change of the elements of $\boldsymbol{\beta}^{(2)}$ upon changing from a gas-phase environment to the liquid phase. Despite the fact that a strong dependence on the molecular configurations used in the calculations has been reported [32], most theoretical

*chungwen.liang@gmail.com

studies have assumed that the water hyperpolarizability tensor elements are constant [26,29–31,33], and thus independent of the inhomogeneous liquid environment or the internal geometry of the water molecule. It should, however, be noted that in the most commonly adopted description, the SHS process is assumed to take place instantaneously, so that each water molecule should respond according to its environment. Only by simultaneously taking into account the structural correlations between molecules [20,33] and the variation of their second-harmonic response would it be possible to reach an approximate quantitative description of SHS experiments.

In this Rapid Communication we investigate the hyperpolarizability of water molecules in the liquid phase, and demonstrate that the inhomogeneous electrostatic environment has a significant impact on the elements of $\boldsymbol{\beta}^{(2)}$. We also consider the role played by thermal and quantum fluctuations of the internal coordinates of each molecule, finding evidence for a significant isotope effect between H_2O and D_2O. Finally, we establish a theoretical framework that allows us to combine a high-level quantum mechanical evaluation of the second-order response with a machine-learning model that can accurately predict the behavior of molecules in large-scale molecular dynamics simulations. We envision that this framework will facilitate the calculation of the full SHS intensity from atomistic simulations, which we leave for future work.

In order to investigate the role of solvent fluctuations in determining the hyperpolarizability of a water molecule in the liquid phase, we use an embedding approach inspired by QM/MM methods, where the hyperpolarizability of a central water molecule is treated quantum mechanically, whereas the surrounding molecules are treated classically. We first perform extensive, long-time, and large-scale molecular dynamics (MD) simulations of bulk liquid water using fixed point-charge models [34,35] see Supplemental Material (SM) [36].

From the results of these simulations, we extract random configurations of water environments by taking molecules within 1.5 nm of a central water molecule. We show in the Supplemental Material that this cutoff is sufficient to provide a representative sampling of the electrostatic environment in bulk water. We perform quantum chemistry calculations of the hyperpolarizability tensor of the central molecule, with the surrounding molecules modeled as point charges consistent with the empirical force field. Since our objective here is to assess the importance of fluctuations on the molecular hyperpolarizability of water, and to develop a computational framework that is compatible with the large-scale simulations needed to model SHS experiments, we limit our discussion to this simple monomer embedding. All hyperpolarizability calculations were performed at the coupled-cluster theory with single and double excitations/doubly augmented correlation-consistent polarized valence triple zeta (CCSD/d-aug-cc-pVTZ) level using the Dalton 2015 package [50]. The hyperpolarizability tensor element β_{ijk} (where the subscript is omitted for clarity) is given by the numerical derivative of the energy U with respect to the external electrostatic fields E_i, E_j, and E_k,

$$\beta_{ijk} = \frac{\partial^3 U}{\partial E_i \partial E_j \partial E_k}. \quad (1)$$

We calculate the static hyperpolarizability tensor, which is an approximation to the full frequency-dependent tensor probed in SHS experiments. For aqueous systems at the frequencies typically used in elastic second-harmonic scattering experiments, this approximation can be expected to entail an error smaller than 10% [30], which should not affect the qualitative scope of our discussion of the assessment and the machine learning of the local fluctuations of $\boldsymbol{\beta}^{(2)}$.

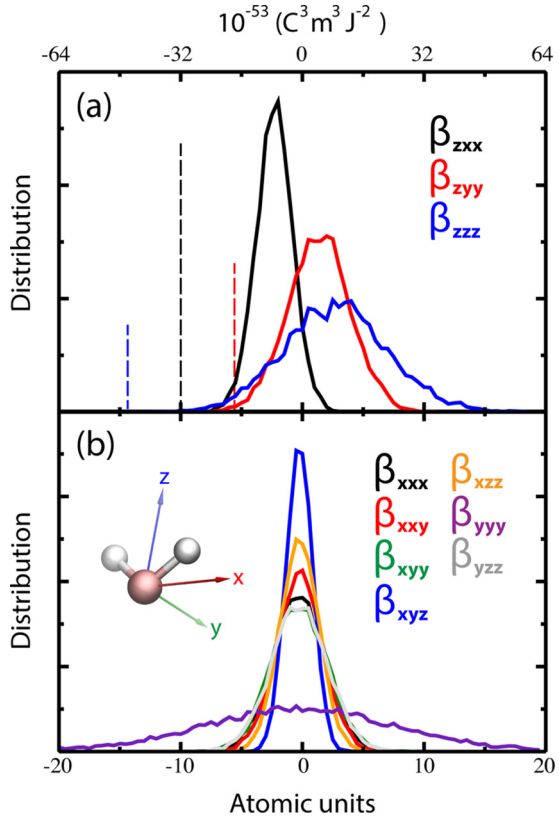

FIG. 1. (a) The distributions of three tensor elements β_{zxx}, β_{zyy}, and β_{zzz}. For comparison, the constant gas-phase values are shown as dashed lines. (b) The distributions of the remaining seven tensor elements for a C_{2v} molecule. Inset: Orientation of the central water molecule.

The distributions of β_{zxx}, β_{zyy}, and β_{zzz} are shown in Fig. 1(a), and compared to the values for a (rigid) gas-phase molecule. It can be seen that these elements have a wide distribution and are shifted towards positive values compared to the gas phase. Both effects are most pronounced for β_{zzz}. Furthermore, it should be noted that most previous studies [22,26,29–31] have focused on calculations of these three elements, which are the only independent, nonzero values considering the C_{2v} symmetry of a water molecule [13,51]. Fluctuations in the liquid phase break this symmetry, so that instantaneously $\boldsymbol{\beta}^{(2)}$ has ten independent nonzero elements. Figure 1(b) shows the distributions of the tensor elements that would be zero under C_{2v} symmetry. While the average of these elements vanishes, their spread is comparable to that of β_{zxx}—and much larger in the case of β_{yyy}—suggesting that these elements may contribute significantly to the total SHS response of aqueous systems. This figure clearly shows that neglecting environmental fluctuations and treating the hyperpolarizability as a constant constitutes a severe approximation, and may have an effect on the interpretation of experiments.

Let us now consider the physical origin of these fluctuations, and of the positive shift of β_{zxx}, β_{zyy}, and β_{zzz}. If one assumes that the overall hyperpolarizability can be described by a Taylor expansion of higher-order polarizabilities which couple with the local electrostatic field, a tensor element $\beta_{ijk}^{\text{liquid}}$ in the liquid phase can be written as

$$\beta_{ijk}^{\text{liquid}} = \beta_{ijk}^{\text{gas}} + \sum_{l=x,y,z} \gamma_{ijkl}^{\text{gas}} E_l, \qquad (2)$$

where $\gamma_{ijkl}^{\text{gas}}$ is the tensor element of the water third-order polarizability ($\boldsymbol{\gamma}^{(3)}$) in the gas phase. E_l is the electrostatic field along the x, y, or z direction evaluated at the position of the O atom of the central water molecule. The contribution of the higher-order hyperpolarizabilities is assumed to be negligible. To rule out contributions from the distortions of each monomer, we will consider snapshots from our simulation of rigid TIP4P/2005 water. $\gamma_{ijkl}^{\text{gas}}$ is calculated based on the geometry of the TIP4P/2005 water model (shown in Table S1). The correlation plots of the values of β_{zxx}, β_{zyy}, and β_{zzz} computed based on the embedded-monomer model, and those estimated from Eq. (2), are shown in Fig. 2(a), together with the distributions of the electrostatic field components, shown in Fig. 2(b). We show in Table S1 that the tensor elements $\gamma_{zxxz}^{\text{gas}}$, $\gamma_{zyyz}^{\text{gas}}$, and $\gamma_{zzzz}^{\text{gas}}$ are large positive numbers, while the other components are near zero. Hence, E_x and E_y contribute negligibly to the shift, while the electrostatic field along the water dipole direction E_z (which generally takes positive values) is predicted to induce a positive shift on the values of

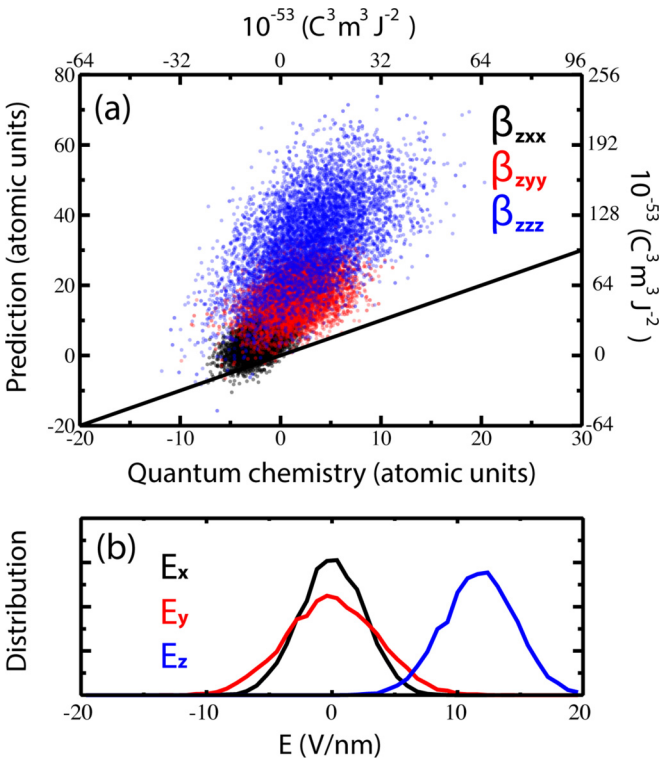

FIG. 2. (a) Correlation plot between the molecular hyperpolarizability elements calculated using quantum chemistry and those estimated using Eq. (2). (b) Probability distribution of electrostatic fields along the x, y, and z directions in the molecular frame.

β_{zxx}, β_{zyy}, and β_{zzz}. Similar considerations also apply to the other elements of $\boldsymbol{\beta}^{(2)}$. For instance, the large fluctuations in β_{yyy} result from the large value of $\gamma_{yyyy}^{\text{gas}}$ and the large spread in E_y. While the values of the gas-phase $\boldsymbol{\gamma}^{(3)}$ and of the local electrostatic field explain the qualitative shift of $\boldsymbol{\beta}^{(2)}$ upon condensation, it is clear that the simple model in Eq. (2) is insufficient to quantitatively predict the molecular response of water.

Before discussing how a more accurate model can be constructed, let us consider how molecular distortions and nuclear quantization affect $\boldsymbol{\beta}^{(2)}$. To this aim, we carry out calculations in the liquid phase with two flexible water models, classical MD simulations with TIP4P/2005-flexible [38] and path-integral MD (PIMD) simulations with q-TIP4P/F [35], which have parametrizations essentially equivalent to the rigid TIP4P/2005, fitted to reproduce the structural and vibrational properties of water with classical and quantum statistics. In order to evaluate high-accuracy reference values for the gas phase, we also perform classical MD and high-order PIMD [47] simulations using the Partridge-Schwenke monomer potential [46]. The details of the classical MD and the PIMD simulations are described in the SM. Following the same procedure as before, we extracted 10 000 water clusters from the trajectories. The mean and the standard deviation of the three tensor elements β_{zxx}, β_{zyy} and β_{zzz} calculated from the TIP4P/2005-flexible and q-TIP4P/F models are shown in Fig. 3. For classical water in both the liquid and in the gas phase, thermal fluctuations of the molecular geometry at 300 K lead to negligible changes in the distribution of the elements of $\boldsymbol{\beta}^{(2)}$. However, when nuclear quantum effects are introduced, the distributions of the $\boldsymbol{\beta}^{(2)}$ tensor elements are considerably broadened, with a standard deviation for the β_{zzz} component of the q-TIP4P/F model that is approximately 30% larger than

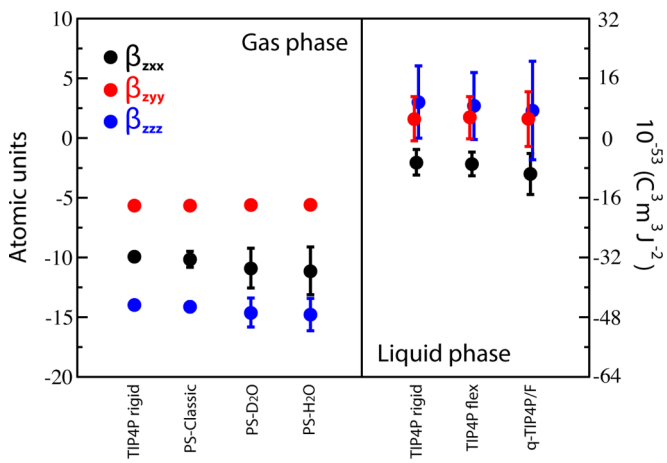

FIG. 3. The mean and standard deviation of three tensor elements β_{zxx}, β_{zyy}, and β_{zzz} calculated in the gas phase with the rigid TIP4P/2005 model for rigid, classical H_2O and the Partridge-Schwenke monomer potential for classical H_2O and quantum D_2O and H_2O, and in the liquid phase with the TIP4P/2005 and TIP4P/2005-flexible models for classical H_2O and with the q-TIP4P/F potential for quantum H_2O. The bars represent the intrinsic variation of the molecular response due to differences in environments and internal distortions. Statistical errors are about 1% of the standard deviation.

its classical counterparts. This observation is consistent with the large changes that are seen in the electronic properties of water when nuclear quantum effects are properly accounted for, e.g., the band gap [52,53] or the H-NMR chemical shifts [54], which are connected to the increased delocalization of the proton along the hydrogen bond.

Significant fluctuations of $\boldsymbol{\beta}^{(2)}$ are also seen for the gas-phase simulations, stressing that internal molecular fluctuations modulate the molecular response, on an ultrafast time scale. From our calculations, we can extract the mean value of $\beta_{\parallel} = \frac{3}{5}(\beta_{zxx} + \beta_{zyy} + \beta_{zzz})$, which is a measurable quantity in electric-field-induced second-harmonic generation (EFISH) experiments [27,28]. The value we obtain, $\langle\beta_{\parallel}\rangle = -18.93(-18.69)$ a.u., for $H_2O(D_2O)$, agree very well with the experimental results reported in Ref. [55] of $-19.2 \pm 0.9(-17.8 \pm 1.2)$ a.u. and in Ref. [28] of -22.0 ± 0.9 a.u. for H_2O. This shows that quantum fluctuations have a pronounced effect on the molecular hyperpolarizability in both the gas and liquid phases. Results for liquid water, $\beta_{\parallel} = 1.53(0.54)$ a.u. for classical (quantum) H_2O, show a significant deviation from the experimental value of 3.19 a.u. [27], but are much closer than the commonly adopted values from fixed environments, which can be as high as 16.3 a.u. [26].

Having assessed the role of quantum fluctuations and that of the inhomogeneous environment in determining the values of $\boldsymbol{\beta}^{(2)}$, we now design a machine-learning model for the prediction of $\boldsymbol{\beta}^{(2)}$ in the liquid phase. This model incorporates the dependence of $\boldsymbol{\beta}^{(2)}$ on the inhomogeneous environment and on quantum fluctuations, and is an essential requirement for the development of a framework to compute the SHS response of liquid water from MD simulations without performing computationally demanding quantum chemistry calculations.

The details of the machine-learning model, including the selection of the training set, the computation of the error, and the selection and the number of fitting parameters are included in the Supplemental Material. However, we report here the main features: We define a grid of points surrounding a central water molecule. Inspired by the observations discussed above, we describe each environment by a vector $\mathbf{u}$ that contains both the electrostatic field generated by all water molecules in the environment, and a smooth Gaussian representation of the oxygen and hydrogen atom densities [56], which accounts for the dependence of the hyperpolarizability on short-range interactions and molecular distortions. We adopt a kernel ridge regression model to learn the hyperpolarizabilities computed from quantum chemistry [57],

$$\beta_{ijk}(\mathbf{u}) = \bar{b}^{(ijk)} + \sum_l c_l^{(ijk)} K(\mathbf{u},\mathbf{u}_l), \tag{3}$$

where we use a Gaussian kernel $K(\mathbf{u},\mathbf{u}') = e^{-|\mathbf{u}-\mathbf{u}'|^2/\sigma^2}$ and optimize the weights $c_l^{(ijk)}$ by minimizing the prediction error for a training set. Once the weights have been determined, one can easily predict the components of $\boldsymbol{\beta}^{(2)}$ using Eq. (3). As shown in Fig. 4, the model can predict the different components of the hyperpolarizability tensor for a test set, with an error of 6%.

In summary, we have demonstrated that the hyperpolarizability $\boldsymbol{\beta}^{(2)}$ of liquid water fluctuates significantly due to the inhomogeneities of the local molecular environment and

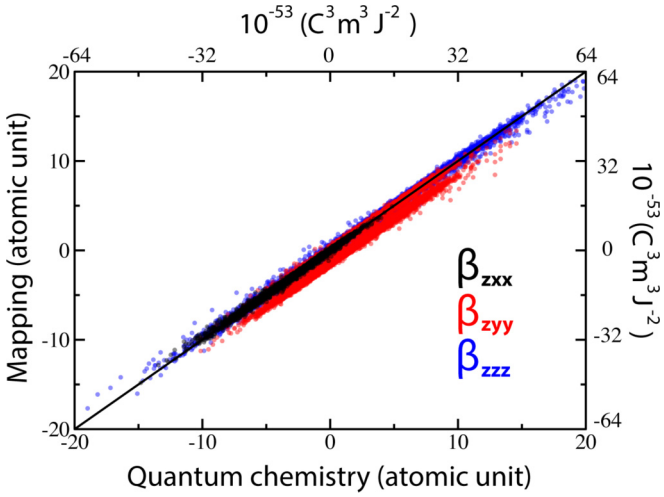

FIG. 4. The correlation plots of β_{zxx}, β_{zyy}, and β_{zzz} between quantum chemistry calculations and the machine-learning mapping procedure.

to nuclear quantum effects. In doing so, we build on previous work that shows the dependence of water's hyperpolarizability on its environment [26,29,30], by explicitly considering the hydrogen-bonding fluctuations of this environment. We see that the assumption of a constant molecular $\boldsymbol{\beta}^{(2)}$, commonly adopted in interpreting SHS experiments, needs to be revised. Fluctuations in the hyperpolarizability enter naturally into the analysis of second-harmonic experiments, because the expression for the second-harmonic intensity contains terms that depend on the square of elements of $\boldsymbol{\beta}^{(2)}$ [3,5]. By providing a quantitative estimate of these fluctuations, our work may aid the interpretation of SHS experiments. Although our results concern bulk water, fluctuations in $\boldsymbol{\beta}^{(2)}$ are present also in interfacial and inhomogeneous systems, which are more relevant to SHG experiments. Including the effects of environmental, geometric, and nuclear quantum fluctuations gives a molecular tensor that agrees much better with the results of the EFISHG experiments than previous work—reaching quantitative agreement in the gas phase. The isotopic dependence of the molecular response is particularly intriguing, as this could contribute to the explanation of recent experimental findings [19] showing that the SHS signal from dilute ionic solutions is largely non-ion-specific, but varies significantly with the isotopic composition of the solvent (H_2O vs D_2O). To achieve quantitative modeling of SHS and answer these questions, it is desirable to calculate the SHS response of the system directly from MD trajectories, going beyond the approximation of a constant molecular response. We take steps towards this goal by introducing a machine-learning framework that can predict the fluctuations in molecular response without needing to resort to expensive, high-level quantum chemistry calculations. It is worth noting that, although we have applied it only to classical and path-integral MD based on empirical force fields, our framework is compatible with any method for sampling configuration space, including simulations in which the nuclear motion is determined by *ab initio* calculations. In addition, although we have considered only bulk water, our framework can be extended to general systems, making it a powerful tool for the

study of interfaces. We show that the full response tensor can be approximated by an embedded-monomer model, although many-body effects are important and could be included as a further refinement. While it is possible to model nanosecond spectroscopic experiments using a constant mean-field value for $\boldsymbol{\beta}^{(2)}$ [20], the realization that on a molecular level the hyperpolarizability reflects the interplay between quantum mechanical and electrostatic fluctuations opens up the possibility of using ultrafast SHS experiments to probe these effects. Future work will involve the quantitative simulation of SHG measurements, which will greatly increase the interpretative power of nonlinear optical experiments of complex aqueous systems, including the study of ion absorption on the water surface [58], the assessment of molecular orientation at the air/water interface [59], and the structure of surfactant molecules interacting with nanoparticles [60].

C.L., G.T., and S.R. are grateful for support from the Julia Jacobi Foundation and the European Research Council (Project No. 616305). D.M.W. and M.C. acknowledge the Swiss National Science Foundation (Project ID 200021_163210). This work was supported by a grant from the Swiss National Supercomputing Centre (CSCS) under Project No. ID s619.

[1] R. W. Boyd, *Nonlinear Optics* (Academic, New York, 2008).
[2] Y. R. Shen, *The Principles of Nonlinear Optics* (Wiley-Interscience, New York, 2002).
[3] Y. R. Shen, Annu. Rev. Phys. Chem. **40**, 327 (1989).
[4] K. Eisenthal, Chem. Rev. **106**, 1462 (2005).
[5] S. Roke and G. Gonella, Annu. Rev. Phys. Chem. **63**, 353 (2012).
[6] R. W. Terhune, P. D. Maker, and C. M. Savage, Phys. Rev. Lett. **14**, 681 (1965).
[7] R. Scheu, B. M. Rankin, Y. Chen, K. C. Jena, D. Ben-Amotz, and S. Roke, Angew. Chem., Int. Ed. **53**, 9560 (2014).
[8] F. M. Geiger, Annu. Rev. Phys. Chem. **60**, 61 (2009).
[9] H. Wang, E. Borguet, and K. B. Eisenthal, J. Phys. Chem. A **101**, 713 (1997).
[10] Y. Liu, J. I. Dadap, D. Zimdars, and K. B. Eisenthal, J. Phys. Chem. B **103**, 2480 (1999).
[11] J. Butet, J. Duboisset, G. Bachelier, I. Russier-Antoine, E. Benichou, C. Jonin, and P. Brevet, Nano Lett. **10**, 1717 (2010).
[12] D. P. Shelton, J. Chem. Phys. **136**, 044503 (2012).
[13] R. Bersohn, Y. H. Pao, and H. L. Frisch, J. Chem. Phys. **45**, 3184 (1966).
[14] V. P. Sokhan and D. J. Tildesley, Mol. Phys. **92**, 625 (1997).
[15] Q. Wan and G. Galli, Phys. Rev. Lett. **115**, 246404 (2015).
[16] M. Kauranen and A. Persoons, J. Chem. Phys. **104**, 3445 (1996).
[17] D. P. Shelton, J. Chem. Phys. **141**, 224506 (2014).
[18] D. P. Shelton, J. Chem. Phys. **143**, 134503 (2015).
[19] Y. Chen, H. I. Okur, N. Gomopoulos, C. Macias-Romero, P. S. Cremer, P. B. Petersen, G. Tocci, D. M. Wilkins, C. Liang, M. Ceriotti, and S. Roke, Sci. Adv. **2**, e1501891 (2016).
[20] G. Tocci, C. Liang, D. M. Wilkins, S. Roke, and M. Ceriotti, J. Phys. Chem. Lett. **7**, 4311 (2016).
[21] H. A. Kurtz, J. J. P. Stewart, and K. M. Dieter, J. Comput. Chem. **11**, 82 (1990).
[22] G. Maroulis, J. Chem. Phys. **94**, 1182 (1991).
[23] H. Sekino and R. J. Bartlett, J. Chem. Phys. **98**, 3022 (1993).
[24] K. V. Mikkelsen, Y. Luo, H. Ågren, and P. Jörgensen, J. Chem. Phys. **100**, 8240 (1994).
[25] S. D. Bella, T. J. Marks, and M. A. Ratner, J. Am. Chem. Soc. **116**, 4440 (1994).
[26] A. V. Gubskaya and P. G. Kusalik, Mol. Phys. **99**, 1107 (2001).
[27] B. F. Levine and C. G. Bethea, J. Chem. Phys. **65**, 2429 (1976).
[28] J. F. Ward and C. K. Miller, Phys. Rev. A **19**, 826 (1979).
[29] J. Kongsted, A. Osted, and K. V. Mikkelsen, J. Chem. Phys. **119**, 10519 (2003).
[30] K. O. Sylvester-Hvid, K. V. Mikkelsen, P. Norman, D. Jonsson, and H. Ågren, J. Phys. Chem. A **108**, 8961 (2004).
[31] L. Jensen, P. T. van Duijnen, and J. G. Snijders, J. Chem. Phys. **119**, 12998 (2003).
[32] V. Garbuio, M. Cascella, and O. Pulci, J. Phys.: Condens. Matter **21**, 033101 (2009).
[33] K. Shiratori, S. Yamaguchi, T. Tahara, and A. Morita, J. Chem. Phys. **138**, 064704 (2013).
[34] J. L. F. Abascal and C. Vega, J. Chem. Phys. **123**, 234505 (2005).
[35] S. Habershon, T. E. Markland, and D. E. Manolopoulos, J. Chem. Phys. **131**, 024501 (2009).
[36] See Supplemental Material at http://link.aps.org/supplemental/10.1103/PhysRevB.96.041407 for the simulation details, including Refs. [13,14,34,35,37–49].
[37] E. Lindahl, B. Hess, and D. van der Spoel, J. Mol. Model. **7**, 306 (2001).
[38] M. A. Gonzalez and J. L. F. Abascal, J. Chem. Phys. **135**, 224516 (2011).
[39] S. Miyamoto and P. A. Kollman, J. Comput. Chem. **13**, 952 (1992).
[40] T. Darden, D. York, and L. Pedersen, J. Chem. Phys. **98**, 10089 (1993).
[41] H. J. C. Berendsen, J. P. M. Postma, A. DiNola, and J. R. Haak, J. Chem. Phys. **81**, 3684 (1984).
[42] G. Bussi, D. Donadio, and M. Parrinello, J. Chem. Phys. **126**, 014101 (2007).
[43] M. Parrinello and A. Rahman, J. Chem. Phys. **80**, 860 (1984).
[44] T. E. Markland and D. E. Manolopoulos, Chem. Phys. Lett. **464**, 256 (2008).
[45] M. Ceriotti, M. Parrinello, T. E. Markland, and D. E. Manolopoulos, J. Chem. Phys. **133**, 124104 (2010).
[46] H. Partridge and D. W. Schwenke, J. Chem. Phys. **106**, 4618 (1997).
[47] V. Kapil, J. Behler, and M. Ceriotti, J. Chem. Phys. **145**, 234103 (2016).
[48] M. Suzuki, Phys. Lett. A **201**, 425 (1995).
[49] S. A. Chin, Phys. Lett. A **226**, 344 (1997).
[50] K. Aidas, C. Angeli, K. L. Bak, V. Bakken, R. B. ad L. Boman, O. Christiansen, R. Cimiraglia, S. Coriani, P. Dahle, E. Dalskov, U. Ekström, T. Enevoldsen, J. J. Eriksen, P. Ettenhuber, B. Fernandez *et al.*, Comput. Chem. Mol. Model. **4**, 269 (2014).

[51] J. A. Giordmaine, Phys. Rev. **138**, A1599 (1965).
[52] F. Giberti, A. A. Hassanali, M. Ceriotti, and M. Parrinello, J. Phys. Chem. B **118**, 13226 (2014).
[53] W. Chen, F. Ambrosio, G. Miceli, and A. Pasquarello, Phys. Rev. Lett. **117**, 186401 (2016).
[54] M. Ceriotti, J. Cuny, M. Parrinello, and D. E. Manolopoulos, Proc. Natl. Acad. Sci. USA **110**, 15591 (2013).
[55] P. Kaatz, E. A. Donley, and D. P. Shelton, J. Chem. Phys. **108**, 849 (1998).
[56] A. P. Bartók, R. Kondor, and G. Csányi, Phys. Rev. B **87**, 184115 (2013).
[57] B. Schölkopf, A. Smola, and K.-R. Müller, Neural Comput. **10**, 1299 (1998).
[58] D. E. Otten, P. R. Shaffer, P. L. Geissler, and R. J. Saykally, Proc. Natl. Acad. Sci. USA **109**, 701 (2012).
[59] A. Kundu, H. Watanabe, S. Yamaguchi, and T. Tahara, J. Phys. Chem. C **117**, 8887 (2013).
[60] Y. You, A. Bloomfield, J. Liu, L. Fu, S. B. Herzon, and E. C. Y. Yan, J. Am. Chem. Soc. **134**, 4264 (2012).